JOURNAL OF MATERIALS SCIENCE 35 (2000) 2659–2674

Correlation of fatigue and creep slow crack growth in a medium density polyethylene pipe material

M. PARSONS, E. V. STEPANOV, A. HILTNER*, E. BAER
Department of Macromolecular Science and the Center for Applied Polymer Research, Case Western Reserve University, Cleveland, OH 44106-7202, USA
E-mail: pah6@po.cwru.edu

The relationship between slow crack propagation in creep and fatigue in a medium density polyethylene pipe material was studied by increasing the R-ratio (defined as the ratio of minimum to maximum stress in the fatigue loading cycle) from 0.1 to 1.0 (creep). The study included characterization of the effects of R-ratio and temperature (21 to 80°C) on the mechanism and kinetics of slow crack propagation. With increasing R-ratio and decreasing temperature, the fracture mode changed from stepwise crack propagation, i.e. crack growth by the sequential formation and breakdown of a craze zone, to a "quasi-continuous" mode of crack growth through the preexisting craze. Despite the change in fracture mode, the damage zone, as characterized by the length of the main craze, shear crazes, and crack tip opening displacement, followed the same dependence on loading parameters, and crack growth rate followed the same kinetics. Crack growth rate (da/dt) was related to the maximum stress intensity factor $K_{I,max}$ and R-ratio by a power law relationship $(da/dt) = B' K_{I,max}^4 (1 + R)^{-6}$. Alternatively, crack growth rate was expressed as $(da/dt) = B\langle K_I^4(t)\rangle_T \beta(\dot{\varepsilon})$ with a creep contribution $B\langle K_I^4(t)\rangle_T$, calculated by averaging the known dependence of creep crack growth rate on stress intensity factor K_I over the period T of the sinusoidal loading curve, and a fatigue acceleration factor $\beta(\dot{\varepsilon})$ that depended on strain rate only. The correlation in crack growth kinetics allowed for extrapolation to creep fracture from short-term fatigue testing. The temperature dependence of crack growth rate was contained in the prefactors B and B'. A change in slope of the Arrhenius plot of B' at 55°C indicated that at least two mechanisms contributed to crack propagation, each dominating in a different temperature region. This implied that a simple extrapolation to ambient temperature creep fracture from elevated temperature tests might not be reliable.

1. Introduction

Prediction of slow crack growth in polyethylene pipes used for natural gas distribution is an example where short-term testing is used to predict long-term performance in the field. To accurately predict long-term failure from short-term tests, the failure mechanism must be maintained while the crack growth kinetics is substantially accelerated. Elevating the test temperature is one method of accelerating failure, and a high temperature creep test (PENT test: ASTM F 1473-94) that reproduces the stepwise failure mechanism observed in the field is intended specifically for predicting long-term failure of gas-pipe resins [1].

However, the latest generation pipe resins are highly creep resistant and the PENT test times are too long for testing in a reasonable amount of time even at high temperature [2, 3]. A room temperature fatigue testing protocol was developed [4–7] that also reproduces the stepwise crack growth mechanism observed in field failures [8, 9], and avoids possible annealing effects that can result from elevated temperature. Fatigue tests on several candidate pipe resins were performed over a range of stresses with an R-ratio, defined as the ratio of minimum to maximum load in the fatigue test, of 0.1. The ranking of slow crack growth resistance in polyethylene pipe resins by fatigue testing followed the same ranking order as in elevated temperature creep tests, and the fatigue tests required up to three orders of magnitude less time [4–6]. However, the parameters that describe fatigue and creep crack growth were not linearly proportional so only a qualitative assessment of long-term creep failure could be made from dynamic fatigue testing [4].

The relationship between fatigue and creep can be quantitatively examined by systematically decreasing the dynamic component of fatigue loading. This is

* Author to whom all correspondence should be addressed.

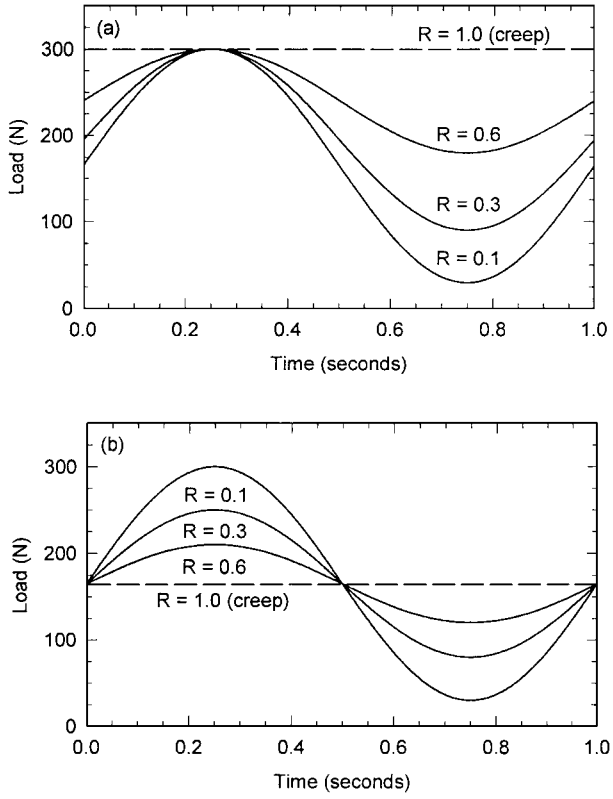

Figure 1 Fatigue loading for different R-ratios under (a) constant $K_{I,max}$ and (b) constant $K_{I,mean}$.

accomplished by varying the R-ratio so that R gradually approaches unity (creep loading). The R-ratio can be varied under conditions of constant maximum load or constant mean load, Fig. 1.

This approach was used to examine the relationship between fatigue and creep in high density polyethylene (HDPE) [10, 11]. Although not a modern pipe resin, HDPE exhibits the stepwise crack propagation mechanism characteristic of field failures and room temperature testing can be done in a reasonable amount of time even in creep loading. Stepwise crack propagation was observed in tests under both constant maximum stress and constant mean stress loading with R-ratios between 0.1 and 1.0 (creep). Crack growth rate in fatigue extrapolated to creep crack growth rate. Conservation of stepwise crack growth and correlation between failure kinetics in fatigue and creep tests suggested that short-term fatigue testing can be used to predict long-term creep failure properties. A power law relation described crack growth rate over the entire range of fatigue and creep loading conditions studied:

$$\frac{da}{dt} = BK_{I,max}^{4.5}K_{I,mean}^{-0.5} = B'K_{I,max}^{4}(1+R)^{-0.5} \quad (1)$$

where $K_{I,max}$ and $K_{I,mean}$ are the maximum and mean stress intensity factors during the fatigue loading cycle. In creep ($K_I = K_{I,max} = K_{I,mean}$), Equation 1 reduces to $da/dt = BK_I^4$, which is consistent with previous observations on creep crack growth in polyethylene [10, 11]. Equation 1 is also consistent with the Paris relationship $da/dt = A\Delta K_I^4$ for fatigue under constant R-ratio ($R < 1$). Equation 1 and the Paris relation can be rewritten as a proportionality between da/dt and $K_{I,max}^4$ or da/dt and $K_{I,mean}^4$ with prefactors that are functions of R only. However, the Paris relation is not expected to hold true for different R-ratios and, indeed, the Paris relation did not fit the data for different R-ratios in slow crack growth in HDPE.

The goal of the present work was to extend the approach used to quantify the relation between fatigue and creep in HDPE to a creep resistant modern polyethylene pipe material. Specimens were cut directly from a medium density polyethylene (MDPE) pipe. Testing was done with varying R-ratio under conditions of constant maximum and constant mean stress loading. Due to the high creep resistance of MDPE pipe, elevated temperatures were also used to accelerate failure. The temperature was varied between room temperature and 80°C, which is the prescribed temperature for the standard PENT creep test. The effects of R-ratio and temperature on the crack growth mechanism and kinetics were examined, and comparison was made to HDPE.

2. Experimental

2.1. MDPE pipe material

Compact tension specimens with dimensions in accordance with ASTM D 5045-93 were cut directly from a medium density polyethylene gas-pipe (MDPE pipe) extruded from category II PE-2406 DuPont Aldyl A resin. The pipe had a 16 inch nominal diameter, the wall thickness was 32 mm, and the thickness to diameter ratio was 13.5. The average density was 0.933 g/cm^3. Schematics illustrating the geometry and dimensions of the compact tension specimens were presented previously [7]. The length, defined as the distance between the line connecting the centers of the loading pin holes and the unnotched outer edge of the specimen, was 26 mm. The height to length ratio was 1.2, and the notch length was 12.5 mm. Specimens were cut in the radial direction parallel to the longitudinal direction of the pipe. The notch extended in the radial direction from the inner pipe wall. Specimens were notched in two steps: the initial 10 mm were made by saw and the final 2.5 mm by razor blade. The razor blade was driven into the specimen at a controlled rate of 1 μm/s. A fresh razor blade was used for each specimen.

2.2. Fatigue and creep testing

Mechanical fatigue units capable of applying a very stable and accurate (±0.5N) sinusoidal load were used to conduct fatigue tests. The units also operated in creep (constant load). The load and crosshead displacement were recorded by computer. A manual zoom macrolens attached to a video camera was used to observe the crack tip. The distance between the lens and the sample was adjusted by a micrometer attachment that enabled direct measurement of the crack length. The camera was routed through a VCR and video monitor and, when the test was left unattended, the experiment was recorded onto video cassette. The maximum and minimum crack tip opening displacement (CTOD), measured at the maximum and minimum stresses in the fatigue loading cycle, were taken from the video. The

TABLE I Matrix of MDPE pipe experiments

T,°C	R-ratio	$K_{I,max}$ MPa(M)$^{1/2}$	$K_{I,mean}$ MPa(m)$^{1/2}$	Fracture mode	$t_{initiation}$ sec $\times 10^3$	$t_{failure}$ sec $\times 10^3$
21	0.1	1.30	0.72	Stepwise	65	250
21	0.2	1.30	0.78	Stepwise	70	320
21	0.3	1.30	0.85	Quasi-continuous (ductile)	75	500
21	0.4	1.30	0.91	Quasi-continuous (ductile)	300	1450
21	0.5	1.30	0.98	Through shear craze	1200	(a)
21	0.6	1.30	1.04	Through shear craze	1700	(a)
21	0.1	0.91	0.50	Stepwise	100	740
21	0.2	0.91	0.55	Stepwise	120	(a)
21	0.3	0.91	0.59	Quasi-continuous	180	(a)
21	0.4	0.91	0.64	Quasi-continuous	1050	(a)
21	0.5	0.91	0.68	Quasi-continuous	2500	(a)
21	0.22	1.17	0.72	Stepwise	80	510
21	0.32	1.09	0.72	Quasi-continuous	200	1220
21	0.43	1.00	0.72	Quasi-continuous	1300	(a)
21	0.1	1.52	0.84	Ductile	—	—
21	0.1	1.43	0.79	Stepwise	62	190
21	0.1	1.08	0.59	Stepwise	78	480
21	0.1	0.78	0.43	Stepwise	120	(a)
21	0.1 (0.5 Hz)	1.30	0.72	Stepwise	135	480
21	0.1 (0.2 Hz)	1.30	0.72	Stepwise	260	960
34	0.1	1.30	0.72	Stepwise	62	(a)
45	0.1	1.30	0.72	Stepwise	56	120
60	0.1	1.30	0.72	Ductile	—	—
60	0.1	1.00	0.55	Stepwise	41	100
60	0.1	0.65	0.36	Stepwise	95	410
70	0.1	0.65	0.36	Stepwise	31	105
80	0.1	0.65	0.36	Stepwise	11	36
80	0.3	0.65	0.43	Stepwise	64	210
80	0.6	0.65	0.52	Stepwise	135	360
80	1.0 (creep)	0.65	0.65	Stepwise	900	(a)
80	0.3	0.55	0.36	Stepwise	55	260
80	0.5	0.48	0.36	Stepwise	155	490
80	0.1	0.78	0.43	Ductile	—	—
80	0.1	0.48	0.26	Stepwise	16	85

(a) Tests stopped before complete failure.

strain rate was obtained from the CTOD measurements as a ratio of the difference between the maximum and minimum values of CTOD and the minimum CTOD in a fatigue cycle, multiplied by the fatigue frequency. Details of the measurement were described previously [11].

Tests were carried out at 21, 35, 45, 60, 70 and 80°C under constant R-ratio, constant $K_{I,max}$, or constant $K_{I,mean}$. The environmental chamber maintained the temperature at ±0.2°C. All experiments are listed in Table I. Under constant maximum stress, R was increased by increasing the minimum stress, Fig. 1a. Under constant mean stress, R was increased by decreasing the maximum stress and increasing the minimum stress, Fig. 1b. At 21°C, two constant maximum stresses of 1.30 and 0.91 MPa(m)$^{1/2}$ and one constant mean stress of 0.72 MPa(m)$^{1/2}$ were used. At 80°C, two constant maximum stresses of 0.65 and 0.48 MPa(m)$^{1/2}$ and one constant mean stress of 0.36 MPa(m)$^{1/2}$ were used. In addition, creep tests on MDPE pipe and HDPE [10, 11] were carried out at 80°C with $K_I = 0.65$ MPa(m)$^{1/2}$. Fatigue tests with constant $R = 0.1$ were performed at 21, 35, 45, 60, 70, and 80°C. Unless noted, the test frequency for fatigue experiments was 1 Hz. The fracture mode, the time to crack initiation ($t_{initiation}$) and the failure time ($t_{failure}$) are also included in Table I.

Fracture surfaces were examined under the light microscope. Features were best resolved in bright field using normal incidence illumination. Specimens were subsequently coated with 9 nm of gold and examined in a JEOL JSM 840A scanning electron microscope. The accelerator voltage was set at 5 kV and the probe current at 6×10^{-11} amps to minimize radiation damage to the specimens.

Selected specimens were loaded to a specific number of cycles, removed from the fatigue unit, and sectioned to obtain a side view of the craze damage zone ahead of the crack tip. Sections were placed on a special SEM sample holder that held the crack open, coated with 9 nm of gold and viewed in the SEM.

2.3. Tensile testing

Yield stress measurements were made on 0.3 mm thick ASTM D 1708 micro-tensile specimens. The specimens were cut from compression molded sheet made from pellets cut from the pipe. The compression molding conditions are described elsewhere [4, 5]. Tensile tests were run on an Instron model 1123 mechanical testing unit at a strain rate of 0.4 sec^{-1}, which was on the order of the strain rate in the fatigue tests [11]. Tests were made at 21, 45, 60, and 80°C.

3. Results and discussion

3.1. Effect of temperature on fatigue crack growth under $R = 0.1$

Increasing temperature lowered the maximum stress for which slow stepwise crack propagation took place. If the stress was too high, rapid ductile fracture occurred. A series of tests determined the effect of temperature on the transition from slow stepwise crack growth to ductile fracture, Fig. 2. The transition occurred at about 1.48, 1.36, 1.15, and 0.75 MPa(m)$^{1/2}$ for temperatures of 21, 45, 60, and 80°C, respectively.

The change in crosshead displacement for slow stepwise crack growth is plotted against time in Fig. 3 for fatigue tests at 21, 45, 60, 70 and 80°C with $R = 0.1$. Corresponding fracture surfaces are shown in Fig. 4. The value of $K_{I,max}$ was 1.30 MPa(m)$^{1/2}$ for the 21 and 45°C tests, and 0.65 MPa(m)$^{1/2}$ for the 60, 70 and 80°C tests. The stepwise character of crack growth, i.e. crack growth resulting from sequential formation and fracture of a craze damage zone ahead of the crack tip, was well resolved on the plots and fracture surfaces for $R = 0.1$. The plateau regions on the plots coincided with crack arrest periods during which a damage zone formed in order to relieve the stress concentration at the crack tip. The duration of the arrest period corresponded to the lifetime of the damage zone. Near the end of the arrest period, the main part of the craze broke down, leaving a continuous membrane at the crack tip. The membrane then ruptured within a few thousand cycles. A sharp increase in crosshead displacement followed membrane rupture. Remnants of broken membrane fibrils made up the prominent striations on the fracture surfaces in Fig. 4. In each test, the number of striations on the surface corresponded to the number of jumps in the plot. The stepwise crack growth mechanism was the same as reported previously in this MDPE pipe material in room temperature fatigue tests [4–7], and was also consistent with observations of stepwise crack growth in elevated temperature creep tests [12]. Comparison of the 21°C test with the 45°C test ($K_{I,max} = 1.30$ MPa(m)$^{1/2}$), and the 60°C test with the 80°C test ($K_{I,max} = 0.65$ MPa(m)$^{1/2}$) revealed that step jump length, defined as the distance between striations, increased with temperature.

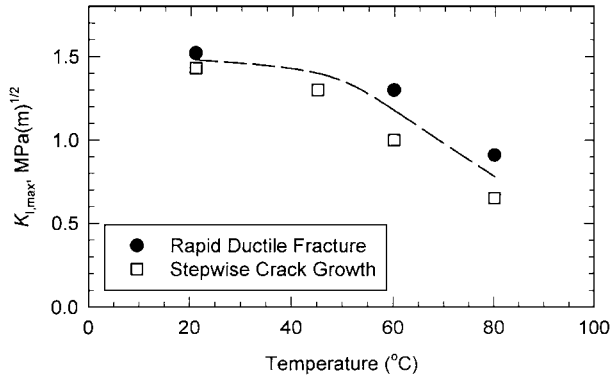

Figure 2 Effect of temperature on the transition from stepwise fracture to ductile fracture for fatigue at $R = 0.1$.

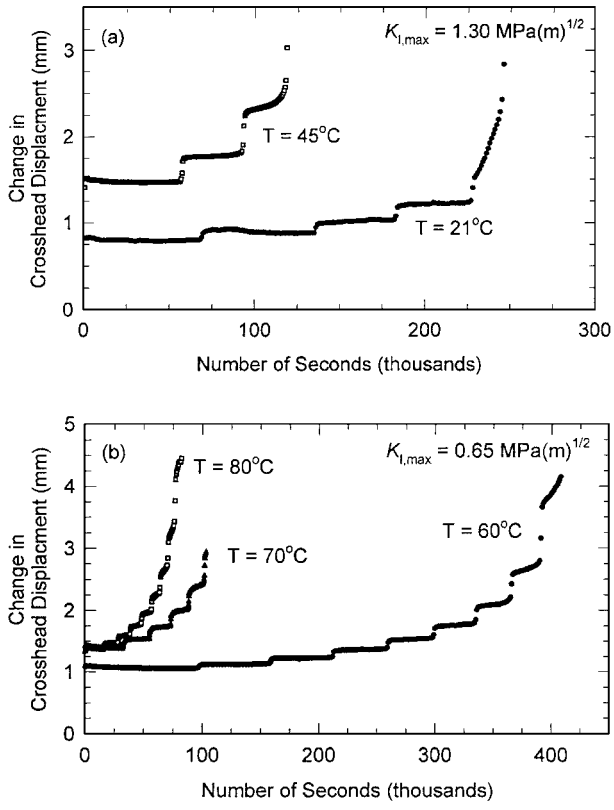

Figure 3 Crosshead displacement curves for stepwise crack growth at $R = 0.1$ for (a) 21 and 45°C at $K_{I,max} = 1.30$ MPa(m)$^{1/2}$ and (b) 60, 70 and 80°C at $K_{I,max} = 0.65$ MPa(m)$^{1/2}$.

In previous experiments on HDPE at 21°C, $K_{I,mean}$ was found to control step jump length [10, 11]. The step jump length is plotted vs. $K_{I,mean}$ for the $R = 0.1$ tests on MDPE pipe at different temperatures in Fig. 5. Step jump length followed a $K^2_{I,mean}$ dependence, which is shown by the curves. This is consistent with the Dugdale model prediction for the length l of the plastic zone at constant load [13, 14]:

$$l = \frac{\pi}{8}\frac{K_I^2}{\sigma_y^2} \tag{2}$$

provided that $K_I = K_{I,mean}$. The temperature dependence of zone length is embodied in the yield stress σ_y. The measured yield stress of MDPE pipe was 19.0, 14.0, 11.4, and 7.4 MPa for $T = 21$, 45, 60, and 80°C, respectively. Substituting these values into Equation 2 not only gave the correct temperature dependence of zone length, but resulted in a prefactor close to $\pi/8$. The exact fit to the Dugdale expression was surprising because, although step jump length in HDPE followed the $K^2_{I,mean}$ dependence, the proportionality coefficient estimated from the step jump length [10] and a yield stress of 29 MPa was greater than $\pi/8$.

Crack growth rate has been proposed as the best parameter to represent crack growth kinetics because it relates directly to the size and lifetime of the damage zone [4–6, 10, 11]. In stepwise crack propagation an average crack growth rate (da/dt) is calculated from the step jump length (da) divided by the lifetime or duration of the damage zone (dt). The rate depends on the stress intensity factor at the crack tip, and increases as the crack grows. This dependence is usually described by the Paris relation [2, 5–7, 15]: $da/dt = A\Delta K_I^n$ where

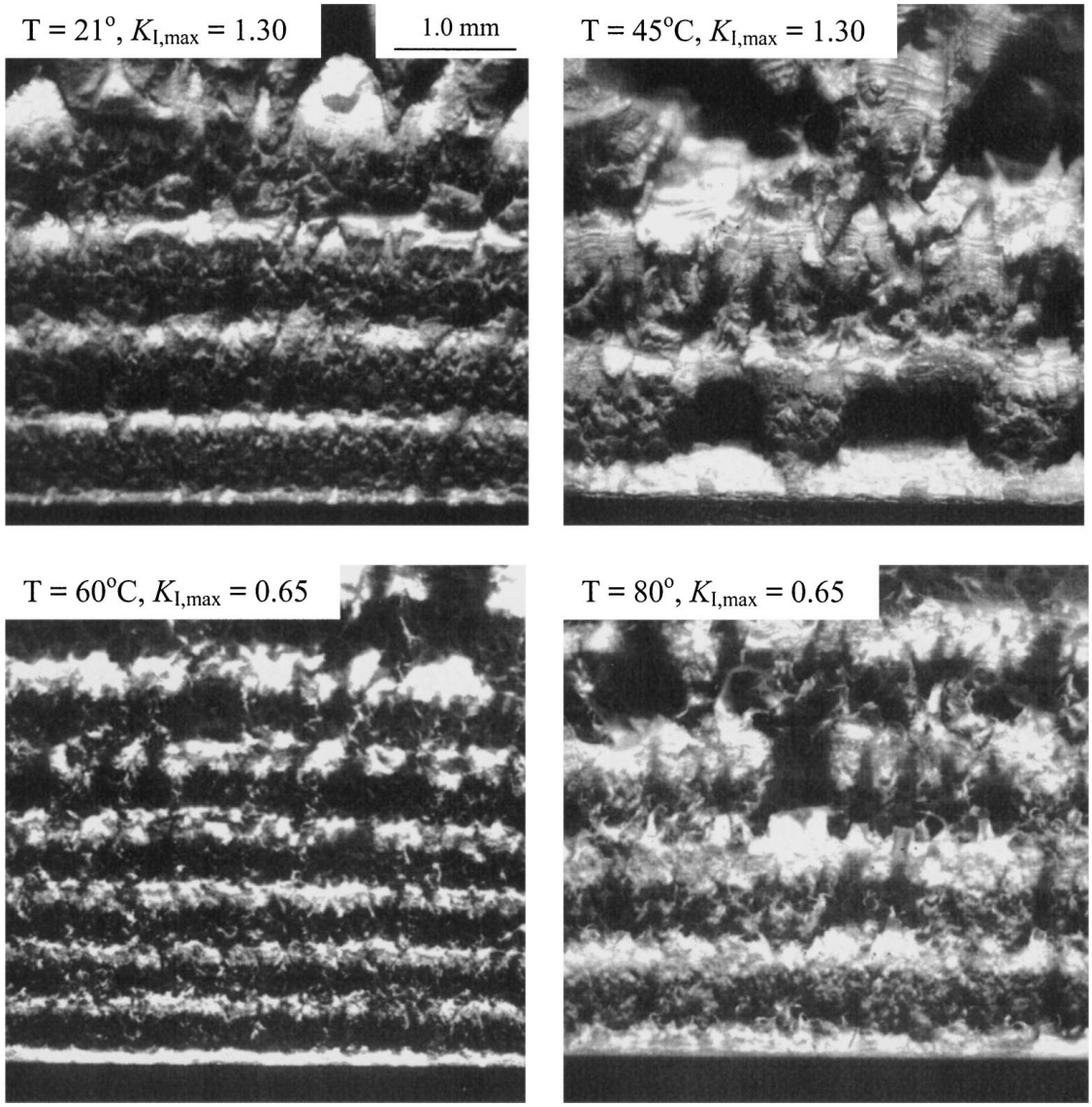

Figure 4 Fracture surfaces of the tests in Fig. 3. $K_{I,max}$ in units of MPa(m)$^{1/2}$.

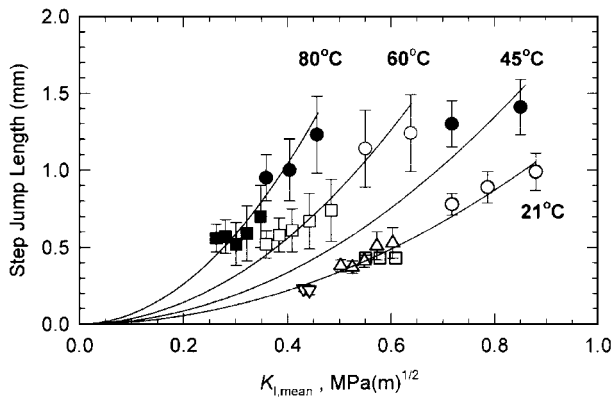

Figure 5 Effect of $K_{I,mean}$ on step jump length at different temperatures for $R = 0.1$. The curves are fits to a $K^2_{I,mean}$ dependence.

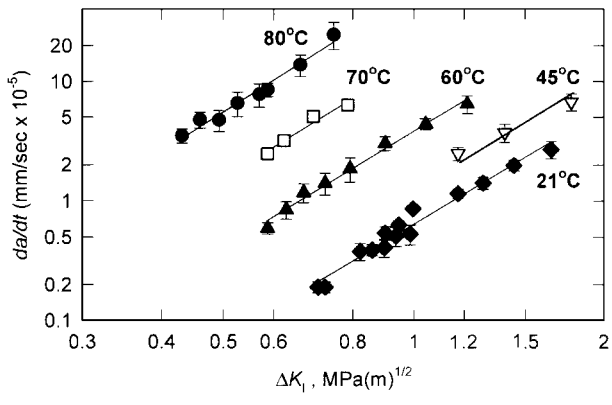

Figure 6 Paris plots of crack growth rate vs. ΔK_I for $R = 0.1$ at different temperatures.

ΔK_I is the difference between the maximum and minimum stress intensity factors in the fatigue loading cycle, and A and n are material constants [16].

Paris plots for tests at constant $R = 0.1$ and $T = 21$, 45, 60, 70 and 80°C are shown in Fig. 6. For all temperatures, crack growth rate followed the Paris relation with an exponent n of 4, which is consistent with previous observations in polyethylene [2, 5–7, 17, 18]. Increasing temperature resulted in a large increase in crack growth rate; for $\Delta K_I = 0.70$ MPa(m)$^{1/2}$ the crack growth rate was 0.18×10^{-5} mm/sec at 21°C and 24×10^{-5} mm/sec at 80°C.

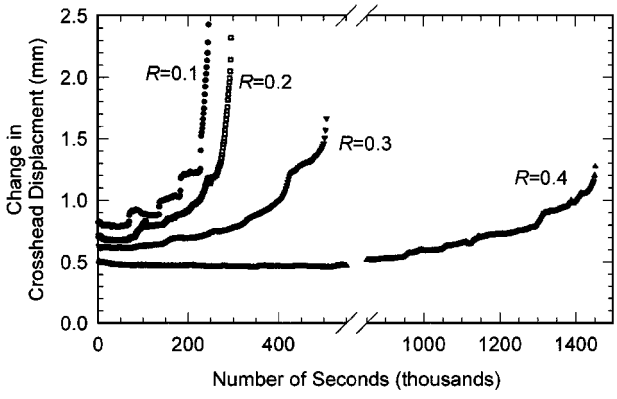

Figure 7 Crosshead displacement curves for fatigue tests at 21°C under different R-ratios with $K_{I,max} = 1.30$ MPa(m)$^{1/2}$.

3.2. Effect of R-ratio on slow crack growth at 21° and 80°C

The effect of varying R-ratio on slow crack growth at 21°C was examined under constant $K_{I,max} = 1.30$ MPa(m)$^{1/2}$ and constant $K_{I,mean} = 0.72$ MPa(m)$^{1/2}$ (Fig. 1). The $R = 0.1$ test corresponded to both conditions: $K_{I,max} = 1.30$ and $K_{I,mean} = 0.72$ MPa(m)$^{1/2}$. Typical crosshead displacement curves for constant $K_{I,max}$ tests are shown in Fig. 7. Fracture surfaces of constant $K_{I,max}$ and constant $K_{I,mean}$ tests are shown in Fig. 8. For $R = 0.2$ under constant $K_{I,max}$ and constant $K_{I,mean}$ loading, step jumps were noticeably shorter and less easily resolved on the fracture surfaces and in the plots than for the $R = 0.1$ test.

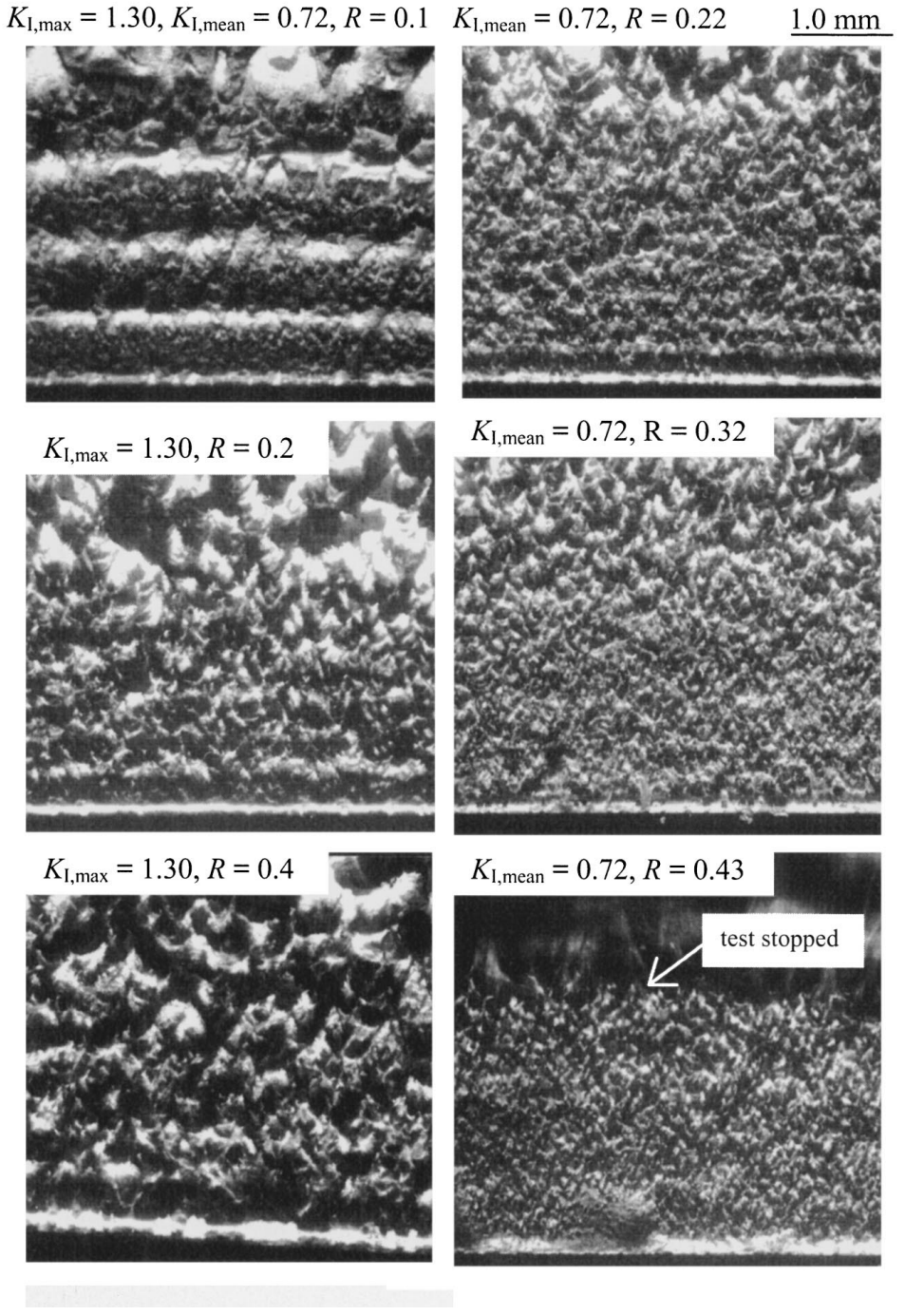

Figure 8 Optical micrographs of fatigue fracture surfaces showing effect of R-ratio for tests under constant $K_{I,max}$ and constant $K_{I,mean}$ loading at 21°C. $K_{I,max}$ and $K_{I,mean}$ in units of MPa(m)$^{1/2}$.

When R-ratio was 0.3 and above, striations were not apparent on the 21°C fracture surfaces. Crack growth under $K_{I,mean} = 0.72$ MPa(m)$^{1/2}$ and $R = 0.32$ and 0.43 began with the formation of voids in the membrane. Craze material was visible directly behind the voids, which indicated that the membrane began to rupture before the main craze fractured. This was in contrast to stepwise crack growth where breakdown of the main craze preceded membrane rupture. The mode of fracture with crack initiation in the membrane and crack growth through the pre-existing craze is termed "quasi-continuous" crack growth. Because the source of the striations on the fracture surfaces in stepwise crack growth was remnants of the highly drawn membrane region that fractured after the main craze, no striations were observed for "quasi-continuous" crack growth.

The SEM micrographs in Fig. 9 show the texture of fractured craze material in the first craze zone. The $R = 0.1$ and 0.2 surfaces had a cellular structure with matted down fibrils and biaxially stretched material. On the other hand, the $R = 0.43$ surface for $K_{I,mean} = 0.43$ MPa(m)$^{1/2}$ was highly fibrillar. Under constant $K_{I,max} = 1.30$ MPa(m)$^{1/2}$ and $R = 0.4$, the surface had a flat, continuous region with numerous micro-striations that extended about 0.3 mm from the notch root. Behind this region the surface consisted of thick, highly drawn fibrils. These features indicated considerable ductile character in the fracture.

An additional series of experiments was run at 21°C with a lower $K_{I,max}$ of 0.91 MPa(m)$^{1/2}$ and R-ratio between 0.1 and 0.4. Low magnification optical micrographs of the fracture surfaces and corresponding SEM micrographs from the first craze zone for $R = 0.1$ and 0.4 are shown in Fig. 10. As was the case for $K_{I,max}$ of 1.30 MPa(m)$^{1/2}$, crack growth was stepwise for $R = 0.1$ and 0.2. Again, step jump length was shorter for $R = 0.2$ (0.20 mm) than for $R = 0.1$ (0.35 mm). For $R = 0.3$ and 0.4, striations were no longer evident on the surfaces and, like the $K_{I,mean}$ loading, "quasi-continuous" crack growth initiated from the crack tip. The $R = 0.1$ surface had the same cellular structure with matted down fibrils and biaxially stretched material that was observed on the other $R = 0.1$ fracture surfaces. When $R = 0.4$, the surface was more fibrillar, Fig. 10.

Tests were also made at 80°C under constant $K_{I,max} = 0.65$ MPa(m)$^{1/2}$ and constant $K_{I,mean} = 0.36$ MPa(m)$^{1/2}$. Crosshead displacement curves and the corresponding fracture surfaces are shown in Figs 11 and 12. In contrast to the room temperature tests, stepwise crack growth was observed for all R-ratios tested, including a creep test at $K_I = 0.65$ MPa(m)$^{1/2}$, with jumps on the crosshead displacement plots and characteristic striations on the fracture surfaces. Under constant $K_{I,max}$, step jump length increased from 1.00 mm for $R = 0.1$ to 1.65 mm for $R = 1.0$ (creep). The increase was less than what was expected for jump length proportional to $K^2_{I,mean}$. Under constant $K_{I,mean} = 0.36$ MPa(m)$^{1/2}$, jump length decreased from 1.00 to 0.70 mm between $R = 0.1$ and 0.5.

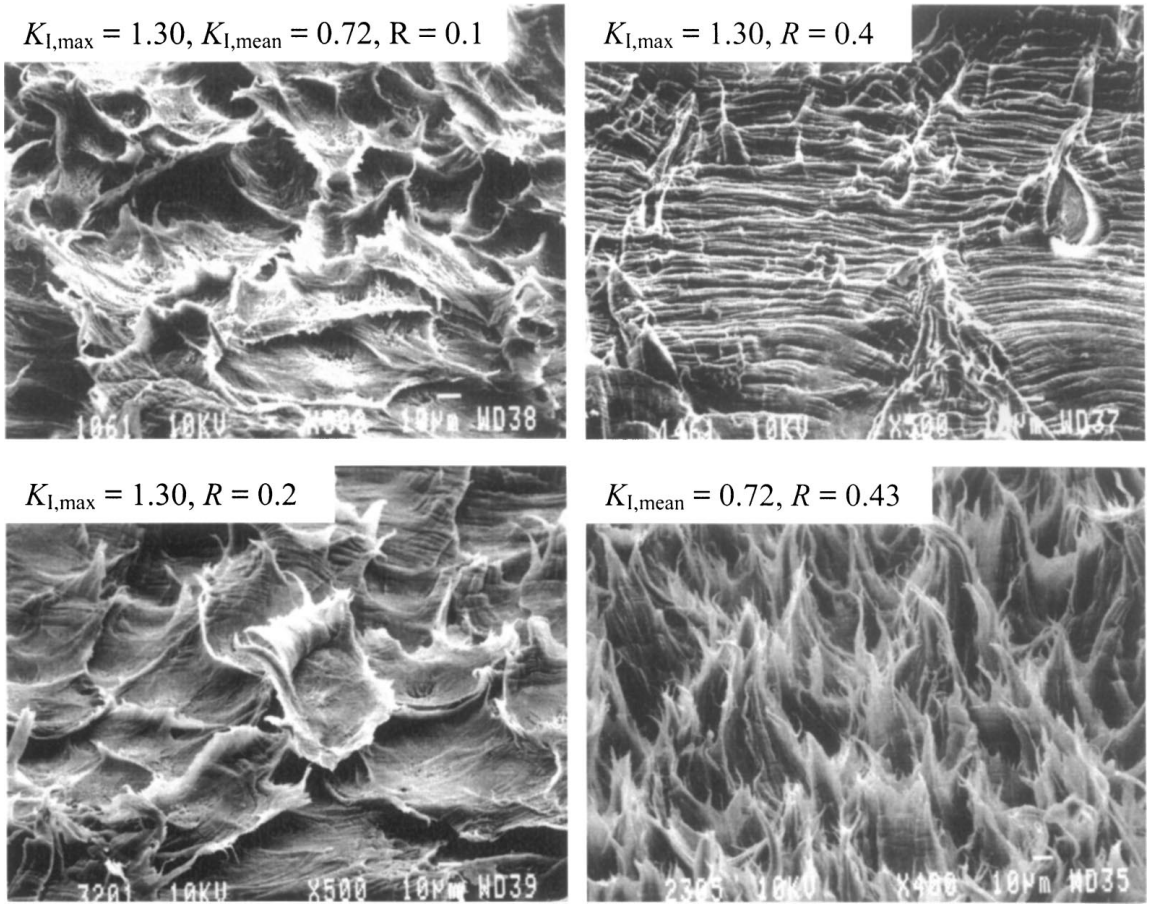

Figure 9 Scanning electron micrographs of the first craze zone of the fracture surfaces in Fig. 8. $K_{I,max}$ and $K_{I,mean}$ in units of MPa(m)$^{1/2}$.

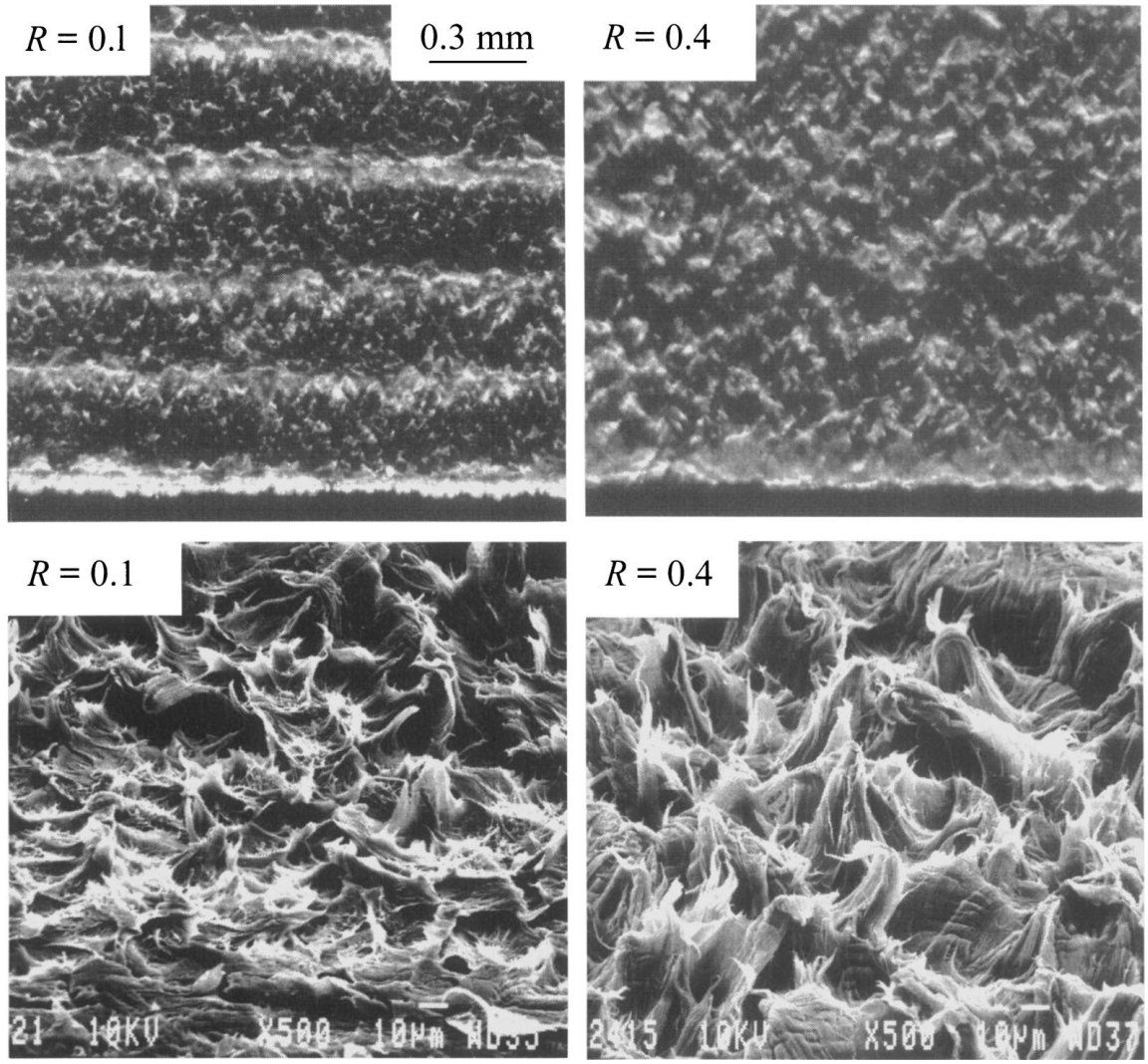

Figure 10 Optical micrographs and scanning electron micrographs of 21°C fatigue fracture surfaces for $K_{I,max} = 0.91$ MPa(m)$^{1/2}$ showing effect of R-ratio.

This contrasted with HDPE where step jump length did not change with R-ratio under constant $K_{I,mean}$ [10, 11].

Higher magnification SEM micrographs from the first craze zone on the fracture surfaces in Fig. 12 are shown in Fig. 13. For $R = 0.1$, the cellular structure with matted down fibrils and biaxially stretched material was observed. With increasing R-ratio the surfaces became more fibrillar, and the fibrils were more highly drawn. For all slow crack growth fractures at 21°C and 80°C under constant $K_{I,max}$ and constant $K_{I,mean}$ loading, the fracture surface became more fibrillar with increasing R-ratio. The fibrillar texture for higher R-ratios resembled the texture of the creep ($R = 1.0$) fracture surface. The change from stepwise to "quasi-continuous" fracture did not correlate with any textural features of the fracture surface, which suggested that the different crack propagation modes did not represent fundamentally different fracture mechanisms.

3.3. Craze fracture

To further characterize the nature of crack growth, formation and fracture of the damage zone ahead of the crack tip were examined. Specimens were loaded for a predetermined number of cycles, removed from the fatigue unit, and sectioned so that a side view of the damage zone was obtained. A typical damage zone, shown in Fig. 14 for a fatigue test under $K_{I,max} = 1.30$ MPa(m)$^{1/2}$ and $R = 0.1$, consisted of a main craze with a continuous membrane at the crack tip; subsidiary shear crazes emerged from the membrane region at an angle of about 30° with respect to the primary craze. In some instances the shear zone consisted of a pair of shear crazes rather than a single shear craze. These features were termed shear crazes because they possessed a cavitated structure although they formed along shear planes, and thereby they represented a combination of crazing and shear banding. Shear crazes have been shown to accompany stepwise crack propagation in polyethylene [4, 12, 19, 20]. The shear crazes together with the primary craze resembled the epsilon-shaped damage zone that is a well-known feature of stepwise fatigue crack propagation in polycarbonate [21]. (However, the shear bands in polycarbonate did not undergo further transformation to the craze-like texture.)

The crack tip opening displacement measured at maximum stress, [$CTOD_{max}$], is also a measure of craze size and, like craze length, was expected to follow a K_I^2 dependence [13, 14]. For tests under varying R-ratio at

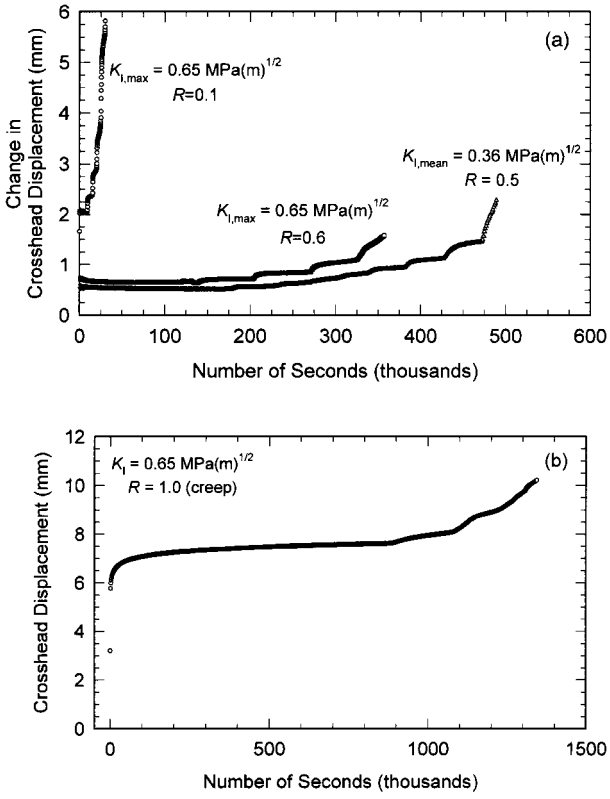

Figure 11 Crosshead displacement curves for (a) fatigue tests at 80°C and (b) a creep test at 80°C.

21 and 80°C, crack tip opening displacement at fracture $[CTOD_{max}]_f$ (the crack tip opening displacement when voids were first observed in the membrane) followed the $K^2_{I,mean}$ dependence, which is shown by the curves in Fig. 15a. Another measure of damage zone size is shear craze length. For the series of tests under constant $K_{I,max} = 1.30$ MPa(m)$^{1/2}$ at 21°C, the length of the shear crazes that accompanied the first craze zone was measured from the side view of the damage zone. Shear craze length, like $[CTOD_{max}]_f$, followed the $K^2_{I,mean}$ dependence, Fig. 15b.

The CTOD and shear craze length measurements suggested that main craze length also followed the expected $K^2_{I,mean}$ dependence. Step jump length, however, did not conform to this expectation. At 21°C under constant $K_{I,max}$ and constant $K_{I,mean}$ loading, step jump length decreased between $R = 0.1$ and 0.2, and steps were no longer observed when R-ratio was 0.3 or greater. This is in contrast to HDPE where stepwise crack propagation was observed over the entire range of R-ratios between 0.1 and 1.0 (creep), and jump length was proportional to $K^2_{I,mean}$ [10, 11]. In MDPE pipe at 80°C, crack growth was stepwise over all R-ratios tested between fatigue and creep, but even in this case jump length did not follow the $K^2_{I,mean}$ dependence. For example, under constant $K_{I,max}$, jump length increased with increasing R-ratio (increasing $K_{I,mean}$), but the increase was less what would be expected with a squared dependence on $K_{I,mean}$. Under constant $K_{I,mean}$, step jump length decreased with increasing R-ratio. Because step jump length was shorter than the $K^2_{I,mean}$ dependence for $R > 0.1$, the crack may have jumped only part way through the zone.

The possibility that step jump length did not correspond to craze length for $R > 0.1$ was confirmed by measuring main craze length in three experiments. Specimens were loaded at 21°C under $K_{I,max} = 1.30$ MPa(m)$^{1/2}$ and $R = 0.1$, 0.2, and 0.3 until just before the crack initiated, i.e. when the damage zone size was at maximum length but before voids were observed in the membrane. Over the small increase in $K_{I,mean}$, the craze length of 0.70, 0.72, and 0.81 mm, for $R = 0.1$, 0.2, and 0.3, respectively, followed the expected $K^2_{I,mean}$ dependence. Step jump length, on the other hand, decreased from about 0.8 to 0.4 mm to zero (quasi-continuous crack growth) over the same range of R-ratios.

The nature of crack growth was examined further by interrupting tests at 21°C after the crack had propagated some distance and examining the crack path, Fig. 16. A test where crack propagation was stepwise ($R = 0.1$ and $K_{I,max} = 1.30$ MPa(m)$^{1/2}$) was stopped after 85,000 cycles, which was well after the first step jump had occurred. In stepwise crack growth, pairs of shear crazes were observed at each successive crack tip. A test where crack growth was "quasi-continuous" ($R = 0.3$ and $K_{I,max} = 0.91$ MPa(m)$^{1/2}$), was stopped at 1,000,000 cycles after the crack reached a length of about 1.5 mm. A pair of shear crazes had formed at the notch tip during the long crack initiation period, but the pairs of shear crazes that marked successive crack tip positions in stepwise crack growth were not observed. Rather, numerous diffuse shear crazes were observed all along the crack path. Shear crazes indicated positions of crack arrest. In "quasi-continuous" crack growth, the crack arrested for only short periods of time, if at all, after crack initiation. Consequently, shear crazes grew only a short distance before the crack advanced and new shear crazes formed at the next crack tip. The result was numerous diffuse shear crazes along the crack. For $R = 0.6$ and $K_{I,max} = 1.30$ MPa(m)$^{1/2}$ a test was stopped after 5,500,000 cycles. The crack did not grow through the main craze. Instead, the crack propagated through one of the shear crazes. An analogous transition from crack growth through the main craze of the epsilon-shaped damage zone to fracture through a shear band was observed with increasing stress in polycarbonate [21]. Under a lower stress of $K_{I,max} = 0.91$ MPa(m)$^{1/2}$ and $R = 0.5$, fracture did not occur through a shear craze but rather through the main craze.

The different crack propagation modes are summarized in the schematic in Fig. 17. With increasing R-ratio toward creep, the fracture mode changed from (a) stepwise crack propagation where the entire main craze fractured before the membrane, to (b) stepwise crack propagation where part of the main craze fractured before the membrane, to (c) "quasi-continuous" slow crack growth where fracture initiated in the membrane, to (d) crack growth through a shear craze. The fracture mode also depended on the stress level because the specimen loaded under $K_{I,max} = 0.91$ MPa(m)$^{1/2}$ and $R = 0.5$ fractured in the "quasi-continuous" mode through the main craze whereas the specimen loaded under $K_{I,max} = 1.30$ MPa(m)$^{1/2}$ and $R = 0.5$ fractured through a shear craze. Indeed, some of the

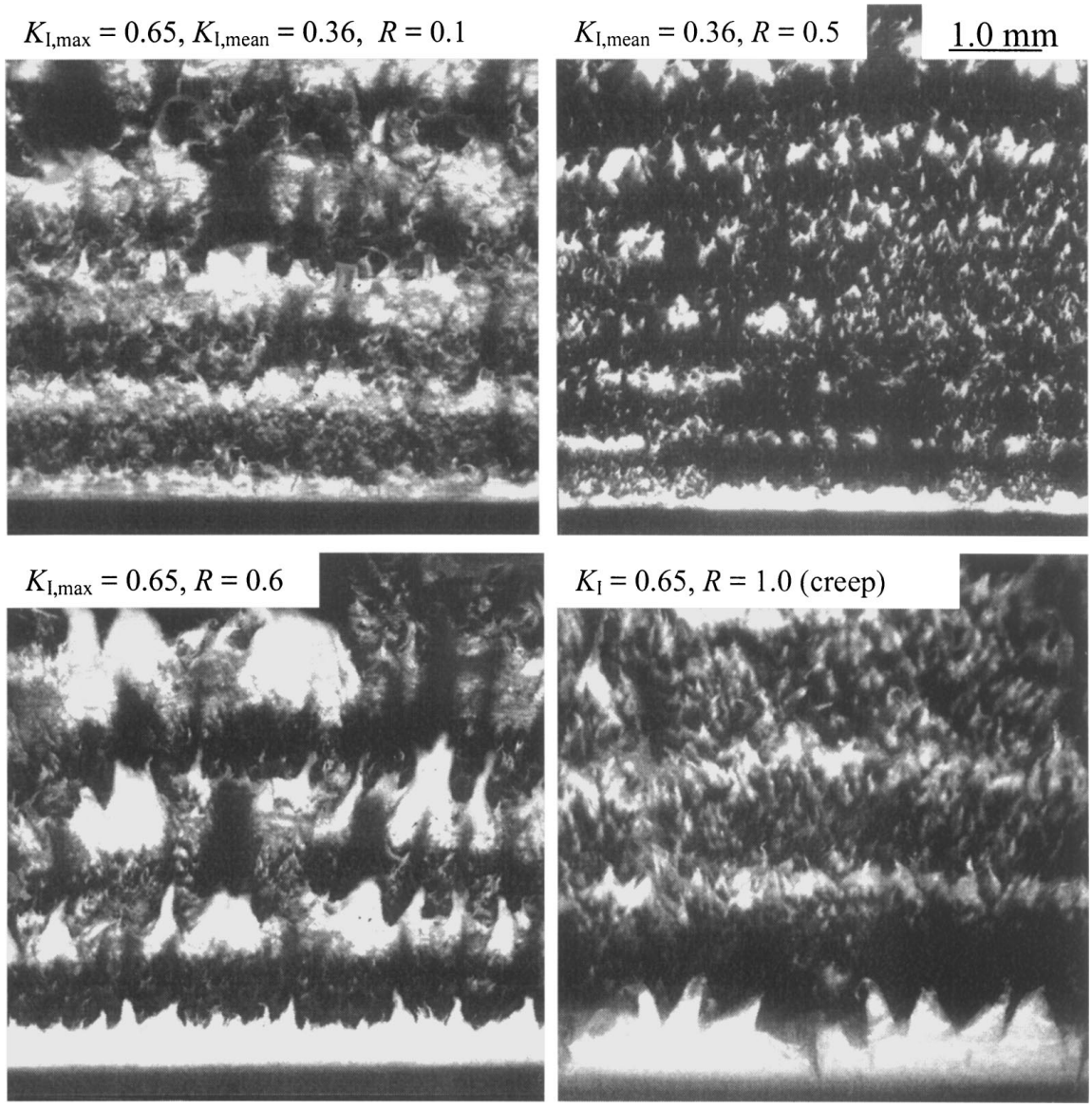

Figure 12 Optical micrographs of the fracture surfaces from the tests at 80°C in Fig. 11. K_I, $K_{I,max}$ and $K_{I,mean}$ in units of MPa(m)$^{1/2}$.

"quasi-continuous" fractures and all the shear craze fractures exhibited ductile fracture features and these tests were not included in the analysis. Increasing temperature had the opposite effect of increasing R-ratio. Increasing temperature to 80°C resulted in all fractures occurring in a stepwise manner where the crack jumped through the entire craze (lower R-ratios) or through part of the craze (higher R-ratios).

Although the fracture mode changed, the damage zone, as characterized by main craze length, shear craze length, and CTOD, followed the Dugdale dependence on $K^2_{I,mean}$. The difference was the location of fracture initiation, i.e., in the main craze or in the membrane at the crack tip. A change in craze fracture mode could result from competition between deterioration of the main craze fibrils and deterioration of the membrane. At low R-ratio where crack propagation was stepwise, the main craze fibrils deteriorated more quickly than the membrane.

The change in crack growth mode with increasing R-ratio may have been a consequence of the high creep crack growth resistance of MDPE pipe. Creep crack growth rate is thought to be controlled by the rate of chain disentanglement in craze fibrils [22–25]. In fatigue, it is speculated that fracture also occurs by chain disentanglement, but fracture is accelerated by a mechanism that is specific to fatigue [26]. In HDPE, which has poor creep resistance, the fatigue crack growth rate at 21°C loading under $R = 0.1$ was 4 to 5 times faster than would be expected if crack growth were completely controlled by the creep process. In MDPE pipe, which has high creep resistance, the contribution of the fatigue component relative to the creep component was much greater. Indeed, when $R = 0.1$, the fatigue crack growth rates in MDPE pipe and HDPE differed by a factor of about 2, whereas in creep the difference was at least an order of magnitude. When R-ratio was increased, the creep component of loading increased and the fatigue component decreased. In MDPE pipe, the highly creep resistant fibrils of the main craze deteriorated more slowly than the membrane, so fracture occurred from the membrane. Conversely, in HDPE, with poor creep resistance of main craze fibrils, stepwise crack propagation was maintained [10, 11]. Increasing temperature accelerated the rate of chain disentanglement in the fibrils, so stepwise crack propagation was

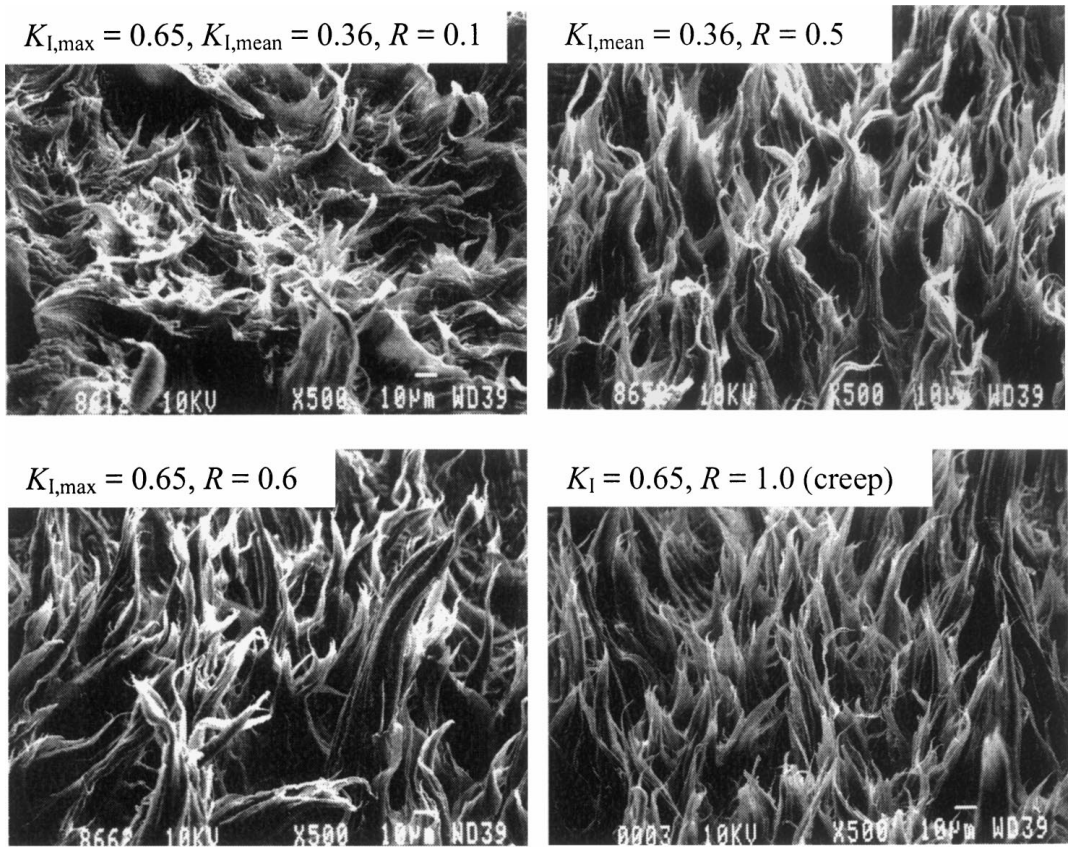

Figure 13 Scanning electron micrographs of the first craze zone of the fracture surfaces in Fig. 12. K_I, $K_{I,max}$ and $K_{I,mean}$ in units of MPa(m)$^{1/2}$.

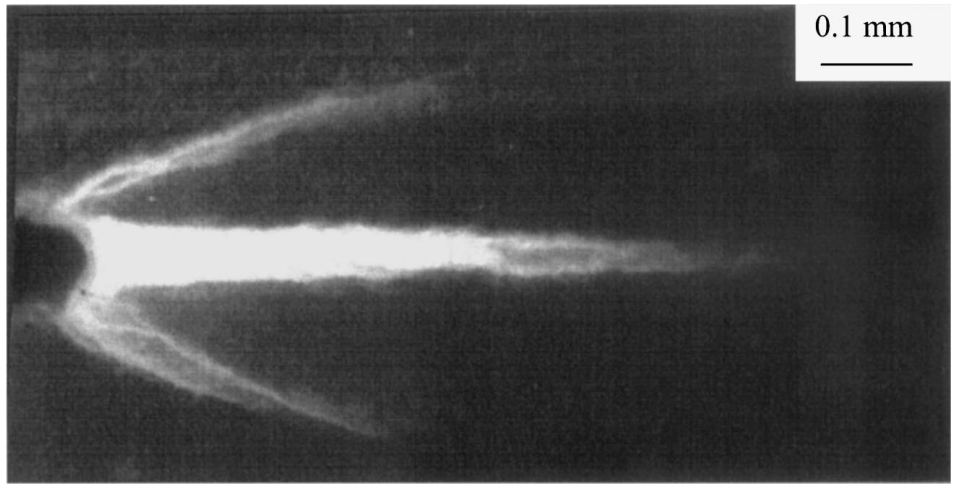

Figure 14 The damage zone in MDPE pipe fatigue loaded at 21°C under $K_{I,max} = 1.30$ MPa(m)$^{1/2}$ and $R = 0.1$.

observed over a larger range of R-ratio. At 80°C crack propagation was stepwise even in creep ($R = 1.0$).

"Quasi-continuous" fracture through the main craze was examined more closely under $K_{I,mean} = 0.72$ MPa(m)$^{1/2}$ and $R = 0.32$. Five specimens were loaded at 21°C to different crack lengths, removed from the fatigue unit, and sectioned to reveal the crack and the craze ahead of the crack. Just before crack initiation, the main craze length was 0.78 mm. The crack initiated at the membrane and grew about 0.3 mm with no appreciable craze growth, i.e. crack growth occurred entirely at the expense of the existing craze. Between 0.3 and 0.6 mm of crack length, both crack and craze grew. Between 0.6 and 0.8 mm of crack length, the craze grew faster than the crack. These data suggested that crack growth and craze growth retained some discontinuous character even though the crack propagated gradually from the membrane rather than by sequential breakdown and formation of a new craze.

Direct measurements of crack length during fatigue tests confirmed the discontinuous character of "quasi-continuous" crack growth. Plots of crack length vs. number of cycles in Fig. 18 show periods of very slow crack growth or possibly crack arrest followed by periods of more rapid crack growth. From these plots, an average crack growth rate was obtained for comparison with crack growth rate in stepwise crack propagation, where the average crack growth rate was obtained

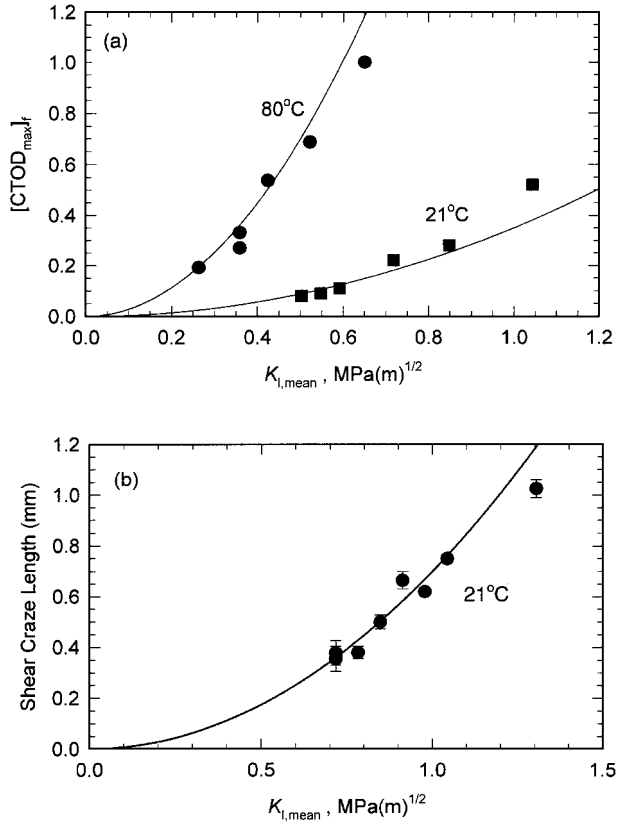

Figure 15 Effect of $K_{I,mean}$ on (a) $[CTOD_{max}]_f$ of the first craze zone and (b) length of shear crazes emanating from the first craze zone. The curves are fits to a $K^2_{I,mean}$ dependence.

from step jump length and duration of the corresponding damage zone.

3.4. Crack growth rate

Crack growth rate is generally accepted as the best way to represent crack resistance of polyethylene resins [4–6, 10, 11], and has been used to compare fatigue crack growth in continuous and discontinuous crack propagation [16]. By varying R-ratio under conditions of constant maximum stress and constant mean stress, the effects of $K_{I,max}$ and $K_{I,mean}$ on crack growth rate can be separated [10, 11]. The effect of $K_{I,mean}$ was obtained by constructing a double logarithmic plot of crack growth rate vs. $K_{I,mean}$ for tests run under constant $K_{I,max}$, Fig. 19a. The regression lines through the data indicated that crack growth rate at 21°C and 80°C followed a $K^{-6}_{I,mean}$ dependence. Similarly, the effect of $K_{I,max}$ was obtained by making a double logarithmic plot of crack growth rate vs. $K_{I,max}$ for tests under constant $K_{I,mean}$, Fig. 19b. The slope of the fit lines indicated that crack growth rate was proportional to $K^{10}_{I,max}$.

Despite the change from crack initiation in the main craze (stepwise crack propagation) to crack initiation at the membrane ("quasi-continuous" crack growth), crack growth rate followed the same relation in each series of experiments. The exceptions were the tests run under $K_{I,max} = 1.30$ MPa(m)$^{1/2}$ with $R = 0.3$ and 0.4. Because the high stress level in these tests approached the transition to ductile crack growth, the crack growth rates were substantially faster than expected from the $K^{-6}_{I,mean}$ dependence. These data were excluded from the analysis.

From the dependencies on $K_{I,max}$ and $K_{I,mean}$ a power law relation in the form:

$$\frac{da}{dt} = B' K^4_{I,max}(1+R)^{-6} \tag{3}$$

described crack growth. The prefactor B' is a material paramater and is a function of temperature. In creep ($K_{I,max} = K_{I,mean} = K_I$) Equation 3 reduces to a proportionality between da/dt and K^4_I, which is consistent with the observed creep crack growth behavior in polyethylene [10, 11, 27–29]. Equation 3 is also consistent with the observations that, under constant $R = 0.1$, fatigue crack growth in MDPE pipe obeys the Paris relation: $da/dt = A\Delta K^{4.0\pm0.5}$ [4, 5]. The fit to $K^4_{I,max}(1+R)^{-6}$ is shown in Fig. 20.

Crack growth rate in MDPE pipe followed the same form as that for HDPE, Equation 1, except the exponents and prefactor were different. A more general form of Equations 1 and 3 is expressed as:

$$\frac{da}{dt} = B' K^m_{I,max}(1+R)^n \tag{4}$$

The parameter m appears to be equal to 4 for all polyethylenes [4, 5, 10, 11, 27–29]. The parameter B' and exponent n are characteristics of the specific resin. The value of B' is 0.72 in MDPE pipe and 0.40 in HDPE, and the exponent n is -6 in MDPE pipe and -0.5 in HDPE. In creep ($R = 1.0$), the expression on the right side of Equation 4 reduces to $(B'/2^n)\ K^m_I$, therefore the parameter B in Equation 1 is $B = (B'/2^n)$ and is a measure of creep crack growth resistance. The term $(1+R)^n$ is a measure of the sensitivity to R-ratio in fatigue.

Varying R-ratio also varies the strain rate $\dot{\varepsilon}$ of craze opening during the fatigue cycle. To include the rate dependency explicitly, an alternative expression for crack growth rate was developed for HDPE [11]:

$$\frac{da}{dt} = B\langle K^4_I(t)\rangle_T \beta(R,\dot{\varepsilon}) \tag{5}$$

where $B\langle K^4_I(t)\rangle_T$ is the creep contribution to the crack growth rate and is obtained by averaging the known dependence of da/dt on K^4_I in creep over the period T of the sinusoidal loading curve [11]. The fatigue acceleration factor $\beta(R,\dot{\varepsilon})$ in HDPE was found to be a linear function of strain rate only: $\beta(\dot{\varepsilon}) = (1 + C\dot{\varepsilon})$. Crack growth rate for MDPE pipe could also be written in this form. The parameter B was calculated from Equation 4 for $R = 1.0$. The strain rate measured for tests under constant R-ratio, constant $K_{I,max}$, and constant $K_{I,mean}$, is plotted against the quantity $(1-R)$ in Fig. 21 for tests at 21°C. The data are plotted against $(1-R) = \Delta K_I/K_{I,max}$ because the amplitudes of the strain and the stress oscillations were expected to correlate. Confirming this expectation, the dependence of strain rate on R was approximately the same for experiments at constant $K_{I,max}$ and constant $K_{I,mean}$. The data were fit with the power law regression $\dot{\varepsilon} = 0.65\ (1-R)^{3.2}$ for strain rate expressed in sec^{-1}.

Using the relationship between R-ratio and strain rate, the crack growth rate normalized to $B\langle K^4_I(t)\rangle_T$ is plotted against strain rate for all fatigue tests at 21°C in

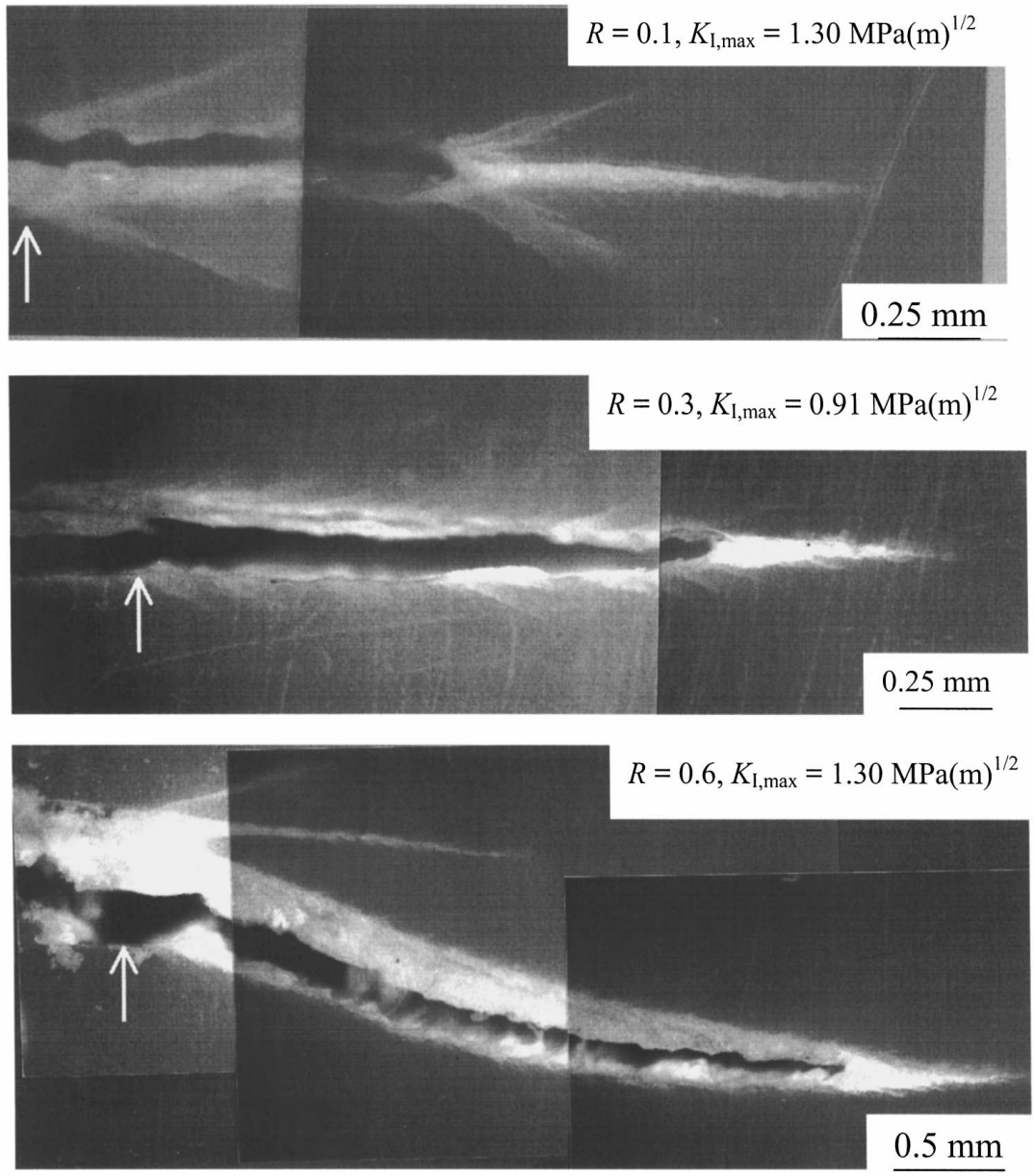

Figure 16 Side views of the crack path in interrupted 21°C fatigue tests showing stepwise, "quasi-continuous", and shear craze crack growth modes.

Fig. 22. (In experiments where strain rate was not measured directly, the regression in Fig. 21 was used.) With some experimental scatter, the data could be considered to fall on the same curve. This indicated that fatigue acceleration of crack growth was primarily a strain rate effect. To confirm this conclusion, additional tests were run with different frequencies (0.5 and 0.2 Hz) under one loading condition ($K_{I,max} = 1.30$ MPa(m)$^{1/2}$ and $R = 0.1$). By varying frequency under a single loading condition, the creep contribution to crack growth remained constant but the strain rate changed. In contrast, both the creep contribution and the strain rate changed when R-ratio was varied. As seen in Fig. 22, the varying frequency data followed the same dependence on strain rate as the data obtained by varying R-ratio. Thus the primary role of strain rate in fatigue acceleration of crack growth is common to HDPE and MDPE pipe resins, and can be suggested as a general effect for polyethylene.

Comparing the values of $B_{HDPE} = 0.57 \times 10^{-5}$ and $B_{MDPE} = 0.011 \times 10^{-5}$ (for crack growth rate expressed in mm/sec) indicates that the MDPE pipe material is about 50 times more resistance to creep crack growth than HDPE. For MDPE pipe as well as for HDPE, the function $\beta(R, \dot{\varepsilon})$ in Equation 5 can be written as a linear function of strain rate only, $\beta(R, \dot{\varepsilon}) = (1 + C\dot{\varepsilon})$. The parameter C is a measure of the strain rate sensitivity in fatigue testing; it has the dimension of time. Comparing the magnitude of this parameter for HDPE [11], $C_{HDPE} = 19$ sec, with that obtained from regression of the data in Fig. 22, $C_{MDPE} = 260$ sec, it is seen that MDPE pipe is much more fatigue sensitive than HDPE. This explains why fatigue crack growth rates in MDPE pipe and HDPE differed by a factor of about 2 when $R = 0.1$ (high strain rate), but reported creep (essentially zero strain rate) lifetimes differed by at least an order of magnitude [2–5]. The difference in creep of MDPE pipe and HDPE may be even larger. For $K_I = 0.65$ MPa(m)$^{1/2}$ the measured creep crack growth rate in HDPE at 80°C was 150×10^{-5} mm/sec, which was about 1,000 times faster than that in MDPE pipe.

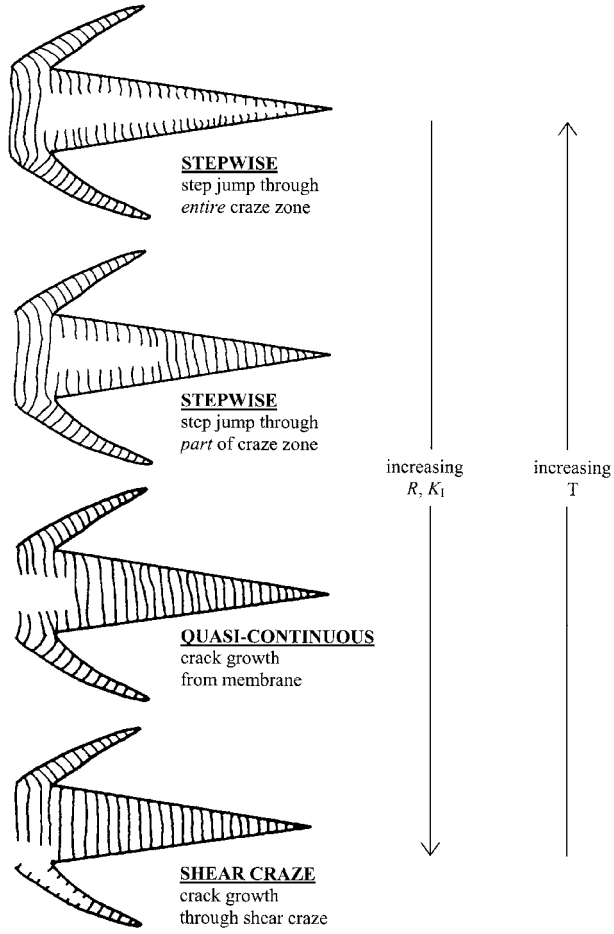

Figure 17 Schematics illustrating the effects of R-ratio, stress and temperature on crack growth mode.

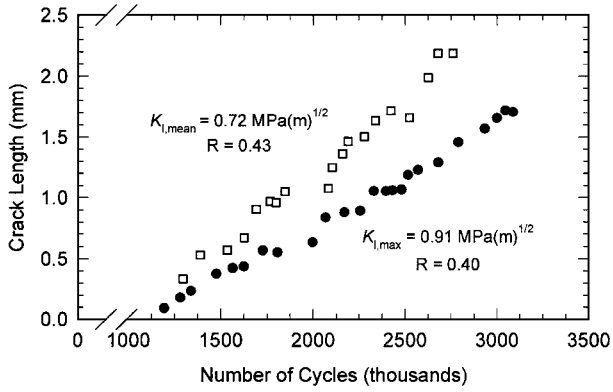

Figure 18 The rate of "quasi-continuous" crack growth in two fatigue tests.

The dependence of strain rate on R-ratio was different in MDPE pipe and HDPE. In MDPE pipe $\dot{\varepsilon} = 0.65\ (1 - R)^{3.2}$ and in HDPE $\dot{\varepsilon} = 0.25\ (1 - R)^{2.0}$. This difference in the exponential dependency of strain rate on the R-ratio term corresponded to the large difference in the exponent n in Equation 4, -6 compared to -0.5. The quantity $(1-R)$ is much more sensitive to a change in power dependence than is the quantity $(1 + R)$ in Equation 3. The different exponential dependency on strain rate (as measured from CTOD) suggested that the crack opened differently in MDPE pipe and HDPE. The shear crazes that emanated from the crack tip in MDPE pipe but not in HDPE are likely to affect the CTOD.

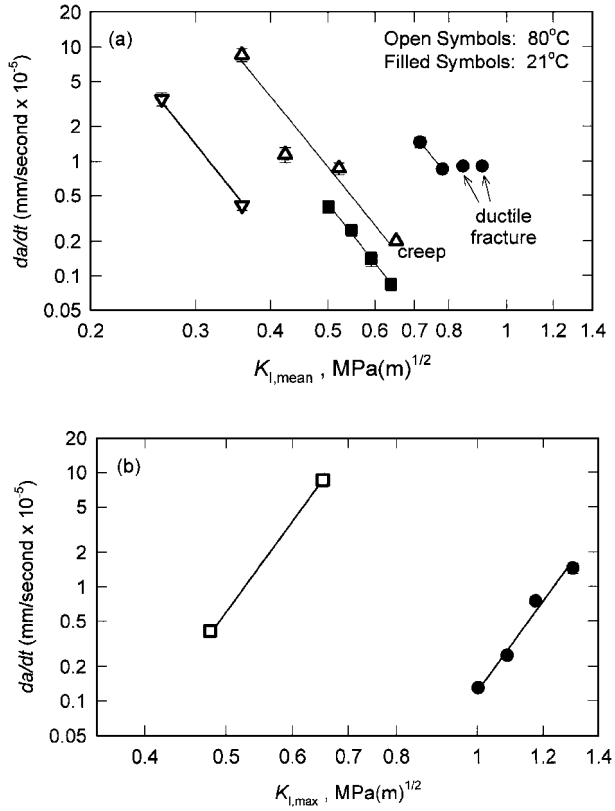

Figure 19 Fits of crack growth rate to (a) $K_{\mathrm{I,mean}}$ and (b) $K_{\mathrm{I,max}}$ for tests at 21 and 80°C.

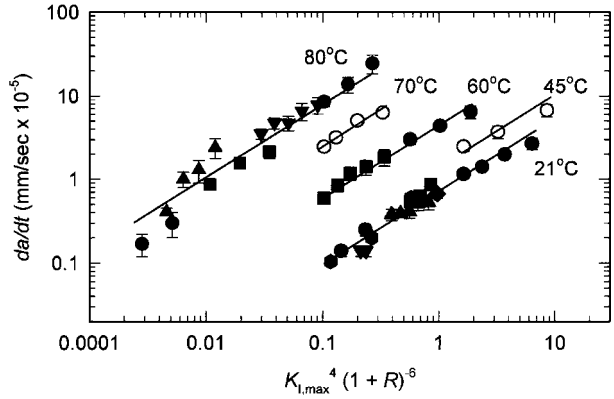

Figure 20 Fit of all crack growth rate data to $K^4_{\mathrm{I,max}}(1 + R)^{-6}$ dependence.

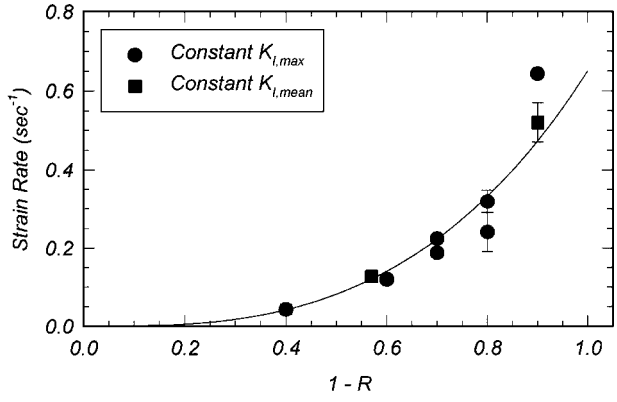

Figure 21 The relation between R-ratio and strain rate at the crack tip at 21°C. The curve is the fit to $\dot{\varepsilon} = 0.65\ (1 - R)^{3.2}$.

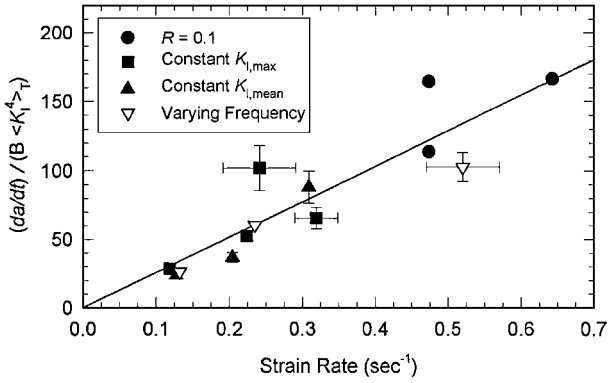

Figure 22 Effect of strain rate on measured crack growth rate normalized to the calculated creep contribution to the crack growth rate at 21°C.

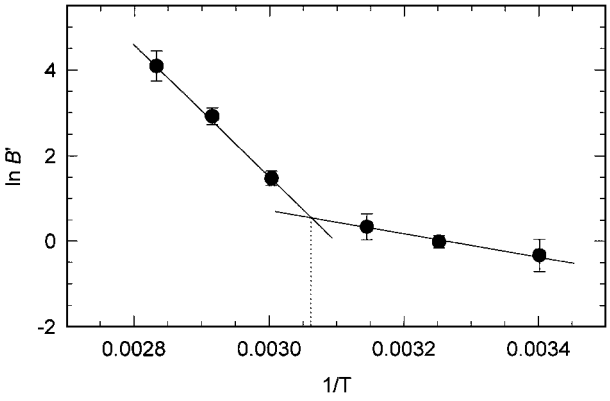

Figure 23 Arrhenius plot of the prefactor B'. The slope change at 55°C is indicated.

The temperature dependence of crack growth rate is contained in the B' term in Equation 4. An Arrhenius plot of ln B' vs. 1/T was constructed to examine this dependence, Fig. 23. The data were described by two straight lines with a slope change at 55°C. For tests between 60 and 80°C, the slope gave an activation energy of about 125 kJ/mol, which is consistent with activation energies obtained in elevated temperature creep tests of MDPE [30, 31]. Below 60°C, however, much lower activation energy of about 25 kJ/mol was obtained. A change in slope at a similar temperature could also be discerned in the transition from stepwise to ductile fracture (Fig. 2). Failure of a single activation energy to describe fatigue and creep crack growth behavior over this relatively small range of temperatures is not surprising considering the complexity of craze growth, damage accumulation, and subsequent craze breakdown processes. Even a simpler case, creep of polyethylene monofilaments between 20°C and 70°C was modeled with two processes differentiated by activation volume [32, 33]. One was associated with the crystalline phase and related to the α-relaxation. The activation energy of 125 kJ/mol obtained from Fig. 23 correlated with the activation energy of this process in polyethylene [33, 34]. Moreover, the temperature of the break in the Arrhenius plot, 50–60°C, corresponded to the maximum of the α-relaxation peak as defined by DMTA loss modulus and dielectric relaxation [34]. The second process was ascribed to the amorphous entanglement network. These different temperature regimes of crack growth rate behavior indicated that a quantitative extrapolation to ambient temperature creep behavior can not be made from elevated temperature tests. Additionally, different polyethylene copolymers might not follow the same dependence on temperature.

4. Conclusions

A damage zone consisting of a main craze with a tough membrane at the crack tip, and subsidiary shear crazes above and below the main craze, formed at the notch root in MDPE pipe for all loads, R-ratios, and temperatures tested. The damage zone dimensions, as characterized by main craze length, shear craze length, and CTOD, followed the Dugdale dependence on $K^2_{I,mean}$. At low R-ratios and high temperatures, crack growth was stepwise, i.e. crack growth occurred by sequential formation and fracture of the main craze. With increasing R-ratio and decreasing temperature, the crack growth mode changed from stepwise to "quasi-continuous" with features of both stepwise and continuous crack propagation. Crack growth rate over the entire range of loading conditions and temperatures examined was related to the maximum stress, R-ratio, and temperature by a power law relation. Alternatively, crack growth rate was modeled as consisting of a creep contribution that was calculated from the sinusoidal loading curve and the known dependence of creep crack growth rate on stress intensity factor, and a fatigue acceleration factor that depended only on strain rate. In comparison to high density polyethylene, MDPE pipe was much more creep resistant, and MDPE pipe was much more sensitive to strain rate in fatigue. The temperature dependence of crack growth rate in MDPE pipe followed an Arrhenius relation with a change in slope at 55°C. The corresponding activation energies were 125 kJ/mol for 80°C $> T >$ 55°C, and 25 kJ/mol for 55°C $> T >$ 21°C. The correlation in crack growth kinetics in tensile-tensile fatigue and creep suggests that short term fatigue testing may be used to predict long term creep fracture properties. However, the change in slope of the Arrhenius temperature dependence of crack growth rate indicates that extrapolation of elevated temperature creep behavior to ambient temperature requires considerable caution.

Acknowledgement

The authors gratefully acknowledge the Gas Research Institute for their financial support of this work.

References

1. N. BROWN and X. LU, in Proceedings of the 12th Plastic Fuel Gas Pipe Symposium, Boston, MA, 1991, p. 128.
2. Y. ZHOU and N. BROWN, *Polym. Eng. Sci.* **33** (1993) 1421.
3. Y. ZHOU, X. LU and N. BROWN, *ibid.* **31** (1991) 711.
4. A. SHAH, E. V. STEPANOV, G. CAPACCIO, A. HILTNER and E. BAER, *J. Polym. Sci: Part B: Polym. Phys.* **36** (1998) 2355.
5. A. SHAH, E. V. STEPANOV, M. KLEIN, A. HILTNER and E. BAER, *J. Mat. Sci.* **33** (1998) 3313.
6. *idem.*, in 1997 Symposium on Plastic Piping Systems for Gas Distribution, Orlando, FL, 1997, p. 235.
7. A. SHAH, E. V. STEPANOV, A. HILTNER, E. BAER and M. KLEIN, *Int. J. Fracture* **84** (1997) 159.

8. K. SEHANOBISH, A. MOET, A. CHUDNOVSKY and P. P. PETRO, *J. Mater. Sci. Lett.* **4** (1985) 890.
9. A. LUSTIGER, M. J. CASSADY, F. S. URALIL and L. E. HULBERT, "Field Failure Reference Catalog for Polyethylene Gas Piping," 1st ed., Gas Research Institute, Chicago, 1986.
10. M. PARSONS, E. V. STEPANOV, A. HILTNER and E. BAER, *J. Mater. Sci.* **34** (1999) 3315.
11. *Idem., ibid.* **35** (2000) 2659.
12. X. LU, R. QUIAN and N. BROWN, *J. Mater. Sci.* **26** (1991) 917.
13. D. S. DUGDALE, *J. Mech. Phys. Solids* **8** (1960) 100.
14. J. R. RICE, in "Fracture, Vol. 2," edited by H. Liebowitz (Academic Press, New York, 1968), p. 191.
15. H. NISHIMURA and I. NARISAWA, *Polym. Eng. Sci.* **31** (1991) 403.
16. R. W. HERTZBERG and J. A. MANSON, "Fatigue of Engineering Plastics" (Academic Press, New York, 1980).
17. Y. Q. ZHOU and N. BROWN, *J. Mater. Sci.* **24** (1989) 1458.
18. H. NISHIMURA, A. NAKASHIBA, M. NAKAKURA and K. SASAI, *Polym. Eng. Sci.* **33** (1993) 895.
19. J. J. STREBEL and A. MOET, *J. Mater. Sci.* **26** (1991) 5671.
20. A. LUSTIGER and R. D. CORNELIUSSEN, *ibid.* **22** (1987) 2470.
21. M. T. TAKEMORI, *Adv. Polym. Sci.* **91/92** (1990) 263.
22. N. BROWN and I. M. WARD, *J. Mater. Sci.* **18** (1983) 1405.
23. B. J. EGAN and O. DELATYCKI, *ibid.* **30** (1995) 3307.
24. X. LU, X. WANG and N. BROWN, *ibid.* **23** (1988) 643.
25. K. FRIEDRICH, *Adv. Polym. Sci.* **52/53** (1983) 225.
26. Y. Q. ZHOU and N. BROWN, *J. Polym. Sci., Part B: Polym. Phys.* **30** (1992) 477.
27. N. BROWN and X. LU, *Polymer* **36** (1995) 543.
28. *Idem., Int. J. Fracture* **69** (1995) 371.
29. P. A. O'CONNELL, M. J. BONNER, R. A. DUCKETT and I. M. WARD, *Polymer* **36** (1995) 2355.
30. Y. L. HUANG and N. BROWN, *J. Mater. Sci.* **23** (1988) 3648.
31. *Idem., J. Polym. Sci., Part B: Polym. Phys.* **28** (1990) 2007.
32. J. RASBURN, P. G. KLEIN and I. M WARD, *ibid.* **32** (1994) 1329.
33. I. M. WARD and M. A. WILDING, *ibid.* **22** (1984) 561.
34. R. H. BOYD, *Polymer* **26** (1985) 323.

Received 5 August
and accepted 28 October 1999